

Optical interconnection using polymer microstructure waveguides

Ray T. Chen, MEMBER SPIE
Physical Optics Corporation
2545 West 237th Street
Torrance, California 90505

Michael R. Wang, MEMBER SPIE
G. J. Sonek, MEMBER SPIE
Physical Optics Corporation
2545 West 237th Street
Torrance, California 90505
and
University of California
Department of Electrical & Computer
Engineering
Irvine, California 92717

Tomasz Jansson, MEMBER SPIE
Physical Optics Corporation
2545 West 237th Street
Torrance, California 90505

Abstract. The properties and development of low-loss (<1 dB/cm) graded-index (GRIN) polymer microstructure waveguides (PMSWs) on various substrates, including semiconductors, conductors, insulators, and ceramics, are described. PMSW films can now be produced, uniformly, over substrate areas exceeding 400 cm². The polymer materials exhibit wide transmission bandwidths (0.3 to 2.7 μ m) and thermal stability characteristics over a large dynamic temperature range (-100°C to +180°C). Local sensitization techniques have been applied to PMSW films to produce planar, single and multiplexed, holographic gratings. Wavelength division demultiplexing devices and single-wavelength 1-to-N fanout optical interconnects have also been realized. The polymer technology reported is well suited for optical interconnection, signal processing, communication, and sensing applications.

Subject terms: optical interconnections, polymer microstructure waveguides, integrated optics, wavelength division multiplexing

Optical Engineering 30(5): 622-628 (May 1991)

CONTENTS

1. Introduction
2. Formation of polymer microstructure waveguides
3. Formation of waveguide holograms by local sensitization with applications to WDM
4. Fanout density and optical interconnection
5. Discussion and applications
6. Conclusions
7. Acknowledgment
8. References

1. INTRODUCTION

The development of advanced optical materials that can focus, multiplex, transmit, modulate, receive, and demultiplex optical signals will be key to the realization of economical and reliable wideband (1-THz) optoelectronic systems for optical signal processing and computing applications. To date, efforts have focused on the development of hybrid and monolithically integrated devices and systems in the LiNbO₃ and GaAs material systems, respectively. A number of technology-related issues, however, currently impede further progress. In particular, both LiNbO₃ and GaAs are incapable of producing the large index modulations that are required to create multiplexed phase gratings, which constitute one of several important building blocks in very large scale optically interconnected systems. Second, the requirements of lattice matching have severely restricted the number and types of materials that can be grown on top of the III-V compound substrates and epilayers. Last, device yields have been relatively low, while costs associated with the growth

and processing of related microstructures have been high. Hence, the development of new, low-cost materials that can be processed into macrostructural optical components, such as waveguides and gratings, will be invaluable to the future optoelectronics integration effort.

In this paper, we report on the development and study of a new polymeric material that overcomes many of the problems associated with the fabrication of conventional macrostructural thin films, as described above, and shows promise for becoming a new, low-cost building block in photonic circuit systems. Polymer microstructure waveguides (PMSWs), which exhibit low loss (0.5 to 1 dB/cm) and excellent optical quality (low defect number), have been formed on a variety of substrates, including GaAs, LiNbO₃, glass, Al, Al₂O₃ and BeO. Recent experimental efforts have also demonstrated PMSWs on Si, quartz, fused silica, phenolic PC board, Cu, Cr, AlN, and Kovar. Optical waveguides with slab guiding layers as large as 20 cm \times 20 cm have been constructed. In addition, the ability to control the refractive index profile of the core guiding region during the fabrication process has been demonstrated. As a result of this refractive index profile tuning capability, fabrication has been possible of low loss polymer waveguide structures on any type of substrate, including semiconductors, conductors, insulators, and ceramics, regardless of the substrate refractive index and loss tangent. A local sensitization technique, used in conjunction with the polymer films, has been developed to facilitate the formation of multiplexed holograms having refractive index modulations as large as 0.2.

2. FORMATION OF POLYMER MICROSTRUCTURE WAVEGUIDES

High-quality thin polymer films, which exhibit propagation losses of less than 1 dB/cm, can be formed from pure photo-lime gelatin

Paper 2898 received Apr. 10, 1990; revised manuscript received Dec. 22, 1990; accepted for publication Dec. 22, 1990.

© 1991 Society of Photo-Optical Instrumentation Engineers

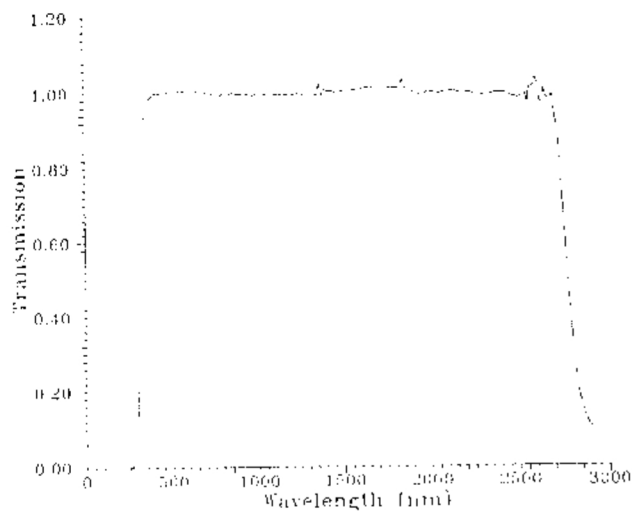


Fig. 1. Transmission spectrum of a 10- μm -thick polymer gelatin thin film.

polymers. When the gelatin is first formed, it exists, in aqueous solution, as a series of single polymer chains surrounded by adjacent water molecules. After standing for a period of time at temperatures below 30°C, solutions containing more than 1% gelatin solidify, forming films that are rigid and, henceforth, rubber-like in their mechanical properties.¹ An optical thin film is formed from the pure photo-lime polymer gelatin by mixing solutions having various gelatin/water ratios, and spinning the solutions on top of a substrate material. By changing the gelatin/water ratio, or the spin speed of film coating, film thicknesses can be achieved that vary from less than 1 μm to greater than 100 μm in dimension. The optical transmission characteristics of a 10- μm -thick gelatin polymer film formed in the above fashion are shown in Fig. 1. Note that the film is nearly 100% transparent from a wavelength of ~ 300 nm to greater than 2700 nm. The above film properties were found to be relatively insensitive to temperature changes. In particular, recent experimental results indicated that the transmission and index properties are stable over the temperature range from -100°C to $+180^\circ\text{C}$ for dry films or holograms prebaked at $+180^\circ\text{C}$. Other tests performed on the polymer films have also indicated a high degree of immunity and radiation hardness to some nuclear and high-power microwave radiation sources. In addition, films prepared in the above manner were previously shown to possess step-index profiles.^{2,3} Their formation on absorptive, or higher index, substrate materials would, therefore, result in the creation of leaky mode waveguides having excessive propagation loss. The influence of substrate loss on guided-wave propagation behavior was experimentally confirmed by depositing polymer films on top of Al_2O_3 and BeO ceramic substrates, respectively, and measuring the mode attenuation via a prism coupling technique. High losses, measured to be in excess of 40 dB/cm, make the step-index polymer films, as processed above, unsuitable for waveguiding applications.

Ideally, the ability to change the index from a step- to a graded-index profile with a higher surface index would enable polymer films to be used on low-loss, as well as extremely lossy, substrate materials. In this case, the lower index portion of the graded-index polymer film would function as a waveguide cladding layer. It would reduce the evanescent field overlap with the underlying substrate and provide tighter mode confinement closer to the polymer film surface. To achieve low-loss wave-

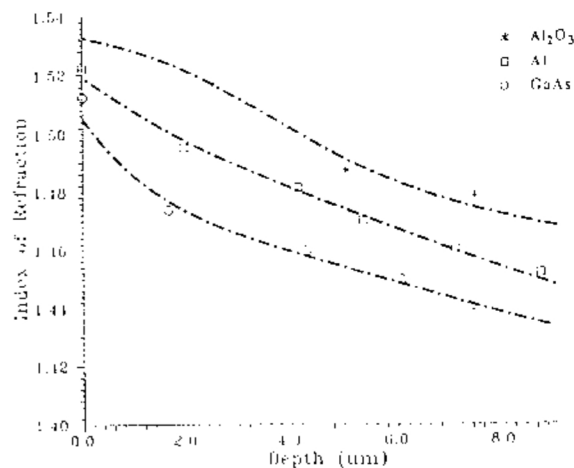


Fig. 2. Refractive index profiles of gelatin polymer films deposited on Al_2O_3 , Al, and GaAs substrates after index tuning. Profile variations are due to differences in film processing parameters rather than substrate-related effects.

guiding in the gelatin films, a method of tuning the refractive index profile from a step-index to a graded-index profile was developed. A combination of systematic wet and dry processing techniques was employed to perturb the mass density of the polymer and, hence, the polymer refractive index. The index of refraction of the newly perturbed polymer film can be qualitatively estimated using the Lorentz-Lorentz formulation⁴ in terms of the average number of molecules, per unit volume, that possess different mass densities. The process of index tuning is actually one of controlled absorption and dehydration. The film is first hardened in a fixer solution and then immersed in a deionized water bath. During this latter step, water absorption causes the film to swell. The process is then reversed by dehydrating the polymer film in a temperature-controlled alcohol bath. To prevent film microcracking, the alcohol concentration is slowly and gradually increased during the final phase of processing. Qualitative data, not shown, but obtained from scanning electron micrographs, indicated that the polymer mass density decreases monotonically toward the substrate surface. High humidity conditions are known to undo the index profile modulation of the film. A detailed study on humidity dependence in a sealed package, and its effects on the transmission and refractive index properties of the polymer film, is currently under way.

Various refractive index profiles for multimode PMSWs, created via the index tuning method, were experimentally measured using the prism coupling technique and analytically determined using the inverse Wentzel-Kramers Brillouin (IWKB) method.^{5,6} The results of these measurements and calculations are shown in Fig. 2 for polymer films that have been deposited on top of Al_2O_3 , Al, and GaAs substrates. Refractive index profiles were calculated by finding solutions to the eigenvalue problem based on a suitable application of the boundary conditions at the waveguide surface. The WKB approximation then yields, as a function of the depth parameter h , the following integral expression for the polymer refractive index⁶:

$$\int_0^{h_q} \left[N^2(h) - N_{\text{eff}q}^2 \right]^{1/2} dh = \frac{4q - 1}{8} \quad q = 1, 2, \dots \quad (1)$$

Here, h is normalized to the free-space wavelength λ ; h_q is defined by the relation $N(h_q) = N_{\text{eff}q}$, $h_0 = 0$, $N_{\text{eff}0} = N(0)$.

and the integral is performed over the extent of the polymer film. The above expression provides an accurate treatment in the present case because the effective index of the zeroth-order mode, within the multimode waveguide, is very close to that of the waveguide surface index. As seen in Fig. 2, a number of different tuned index profiles can be achieved³ through careful control of the polymer absorption and dehydration process. We note that the profile variations on the three different substrates result from differences in process parameters rather than from substrate-related dependences. In all cases, a reduction in the overlap between guided-mode evanescent field and the underlying substrate, due to the presence of a graded-index profile, resulted in the observation of strong waveguiding and propagation losses of 0.5 to 1 dB/cm in the PMSWs. Low-loss waveguiding is also depicted in Fig. 3 for polymer films deposited in GaAs, quartz, glass, Au, and Al₂O₃. Similar results have been observed for gelatin polymers deposited onto other substrate materials, including Si, LiNbO₃, fused silica, Al, Cu, Cr, Kovar, BeO, AlN, and phenolic PC board, respectively. Without the use of special adhesion promoters or surface planarizing layers, the majority of polymer films displayed excellent deposition and adhesion properties on most of the substrates described above. There are no observed effects on the substrate materials described above due to the presence of the polymer layer and the associated chemical processing techniques. However, the presence of the polymer film does change the cover layer index from 1.0 (air) to ~1.53, which, in turn, can affect the waveguiding properties in underlying waveguides such as

ion-exchanged glass waveguides and Ti:indiffused LiNbO₃ waveguides.

3. FORMATION OF WAVEGUIDE HOLOGRAMS BY LOCAL SENSITIZATION WITH APPLICATIONS TO WDM

The formation of tuned index polymer waveguides on virtually any kind of substrate, as described above, provides the basis for the development of other passive optical devices that are suitable for signal routing and modulation. In particular, devices that utilize multiplexed holograms, for wavelength multiplexing and demultiplexing operations, are key components for advanced optical interconnection architectures. Based on the refractive index tuning capability within the polymer film, microlithographic techniques were used in conjunction with a local sensitization process to generate *N*-channel multiplexed holograms. After the polymer film was deposited and cured on top of a suitable substrate, a photoresist window was defined using standard photolithography. Local sensitization was then achieved by immersing the selectively masked sample into a room-temperature ammonium dichromate (DCG) solution.⁷ The masking material was then removed, and within 2 h after drying and stabilization of the sensitized region, the sample was ready for holographic recording and processing.

A similar process was used to form multiplexed holographic phase gratings in the PMSW films. The gratings were created by successively exposing holographic patterns within the selectively defined and sensitized regions of the waveguide. A two-beam interference recording method was used to define individual holographic gratings, each at a different recording angle, and each having a sinusoidal phase modulation profile, such that:

$$K_i = 2k_{\lambda_i} \sin\left(\frac{\alpha_i}{2}\right), \quad (2)$$

where k_{λ_i} and K_i are defined as

$$k_{\lambda_i} = N_{\text{eff},\lambda_i} \frac{2\pi}{\lambda_i}, \quad (3)$$

$$K_i = \frac{2\pi}{\Lambda_i}, \quad (4)$$

where

- α_i = angle of Bragg diffraction
- Λ_i = *i*'th holographic grating period
- K_i = *i*'th grating wave vector
- N_{eff,λ_i} = waveguide mode effective index at λ_i .

The resultant grating wave vector for each hologram lies within a plane that is parallel to the waveguide surface. A schematic of the locally sensitized polymer waveguide, containing a DCG holographic phase grating, is depicted in Fig. 4.

The above technique was used to develop a four-channel wavelength division demultiplexer (WDDM) that operates at the center wavelengths of 632.8 nm (red), 611.9 nm (orange), 594.1 nm (yellow), and 543.0 nm (green).⁸ The device, consisting of a locally sensitized single-mode PMSW and prepared on a soda-lime glass substrate, is shown in Fig. 5. Only the TE₀ guided mode of the waveguide is excited via the prism coupler and utilized in the present device. Holographic recording angles

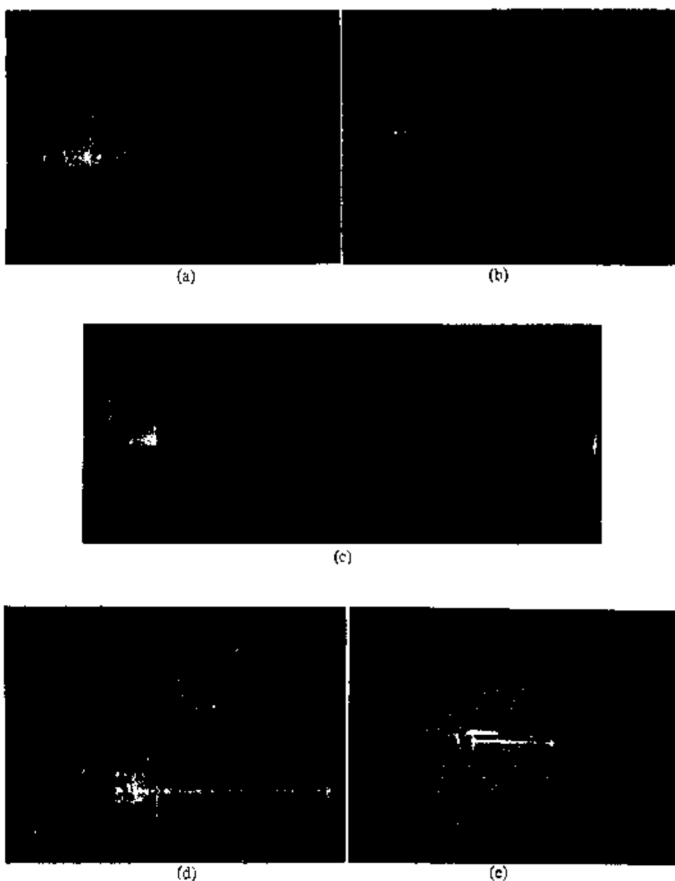


Fig. 3. Optical waveguiding in PMSW films deposited on (a) GaAs, (b) quartz, (c) 20-cm glass, (d) Au, and (e) Al₂O₃ substrates. Profile tuning reduces propagation losses by >40 dB/cm.

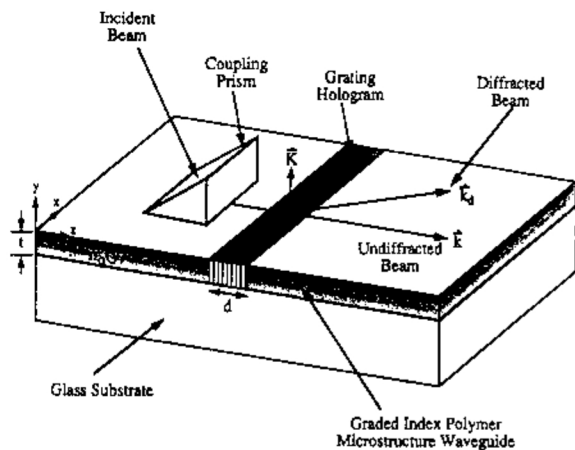


Fig. 4. Schematic of a locally sensitized polymer waveguide containing a DCG holographic phase grating. For multiplexed devices, phase gratings have different Bragg conditions are reexposed within the same sensitized region.

for each of the deflected wavelengths were chosen, commensurate with the effective index dispersion relations of the polymer film. The Bragg diffraction angle of each resulting transmission phase grating was designed to satisfy the phase-matching condition for the signal wavelength of interest. Exposure parameters were adjusted during successive holographic recordings in an attempt to optimize diffraction efficiencies. Each grating was, therefore, designed to be capable of deflecting only one wavelength within a 4- to 10-nm spectral bandwidth. Device measurements yielded a crosstalk figure of less than -40 dB between adjacent channels and a corresponding diffraction efficiency of better than 50% at each wavelength. The angular and spectral sensitivities for the demultiplexer were theoretically determined to be within 0.2 to 0.4°, and ~4 to 10 nm, respectively. It is expected that even higher diffraction efficiencies for each grating can be achieved if the grating modulation index and the interaction length are optimized accordingly. In addition, while excellent crosstalk figures were obtained for the present waveguide demultiplexer, it is conceivable that the presence of substrate radiation modes from each signal carrier, generated by interaction with other existing gratings, could limit the overall device efficiency for closely spaced channels. These modes might be present as a consequence of random fluctuations in the grating modulation index and waveguide thickness, or from variations in the tuned refractive index profile. Some of these issues are discussed in further detail in the following section.

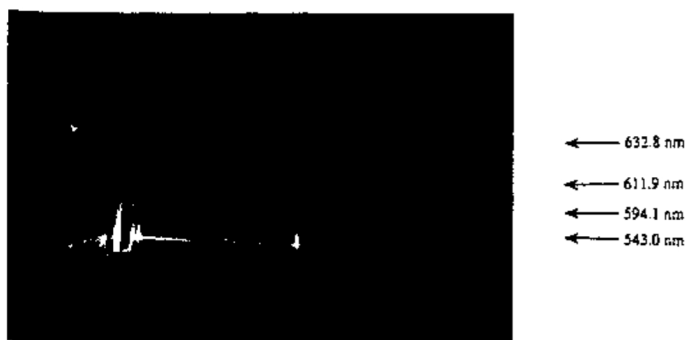


Fig. 5. A four-channel wavelength division demultiplexer using locally sensitized PMSWs. The diffracted wavelengths are 632.8, 611.9, 594.1, and 543.0 nm.

4. FANOUT DENSITY AND OPTICAL INTERCONNECTION

The techniques used to develop the four-channel demultiplexer of Fig. 5 can also be used to create 1-to- N fanout elements for optical interconnection. Such elements will undoubtedly require high efficiencies and low channel crosstalk. Improvements in diffraction efficiency can be expected through careful control of the phase grating parameters, while enhancements in crosstalk figures will depend on the ability to achieve minimal angular overlap between adjacent fanout directions. The modulation index of the polymer film, and its dependence on exposure flux, will ultimately determine the maximum number of phase gratings that can be exposed within a given region of the PMSW, as well as the overall DCG grating efficiency.

Using coupled mode theory as it applies to a lossless step-index waveguide medium containing slanted phase gratings,^{9,10} the diffraction efficiency and the angular and wavelength selectivities can be determined as a function of grating and waveguide parameters, including the interaction length d , index modulation Δn , and overlap integral, for the TE mode of the waveguide. The diffraction efficiency is given by the expression:

$$\eta = \frac{4\kappa^2(\hat{r} \cdot \hat{s})^2}{C_r \delta^2 + 4\kappa^2(\hat{r} \cdot \hat{s})^2} \sin^2 \left\{ \frac{1}{2} \left[\frac{\delta^2}{C_s^2} + \frac{4\kappa^2(\hat{r} \cdot \hat{s})^2}{C_r C_s} \right]^{1/2} d \right\}, \quad (5)$$

where

$$C_r = \beta_{mz} / \beta_m,$$

$$C_s = \sigma_z / \beta_l,$$

$$\delta = (\beta_l^2 - \sigma^2) / 2\beta_l, \quad (6)$$

$$\sigma = \beta_m + \mathbf{K}, \quad (7)$$

$$\kappa = \frac{2\pi^2}{\lambda^2} \int_{-\infty}^{\infty} n_0(y) \Delta n(y) E_m(y) E_l(y) dy, \quad (8)$$

where \hat{r} and \hat{s} are the unit polarization vectors, β_m and β_l are the propagation constants of the incident and diffracted guided modes, and \mathbf{K} is the grating wave vector, respectively. We use σ as the propagation constant of the diffracted mode, and introduce a small dephasing constant δ , as in Eq. (6), to characterize the angular and wavelength selectives of our planar hologram. The Bragg condition is given in Eq. (7), which can be used to determine the diffraction angle and the constant σ . Equation (8) gives the coupling strength, which depends on the overlap between the incident guided mode profile $E_m(y)$, the diffracted guided mode profile $E_l(y)$ and the grating index profiles, $n_0(y)$ and $\Delta n(y)$ (Fig. 4). The terms $E_m(y)$ and $E_l(y)$ satisfy the orthogonality relationship:

$$\int_{-\infty}^{\infty} E_m(y) E_l(y) dy = \frac{\delta_{m,l}}{\beta_m} \quad m, l = 0, 1, 2, \dots \quad (9)$$

For the calculation, complete overlap is assumed between the guided mode and the index perturbation, and the modulation index for each individual grating is assumed to have a value of $\Delta n \sim 0.01$. We note that the effects of having a finite laser

beam width and a graded refractive index profile have not been accounted for in the present analysis. Additional losses that might have been introduced during the DCG sensitization process have similarly been neglected. As expected, the diffraction efficiency of the induced transmission hologram undergoes a periodic transition between a maximum and a minimum value, as the diffraction angle is changed. The diffraction efficiency of each individual waveguide hologram can be improved by changing the exposure dosage during the recording process.^{7,11} The modulation index, as a function of exposure time T_i for the i 'th hologram, can be determined from the expression:

$$\Delta n_i = \left(\Delta n_{\max} - \sum_{j=1}^{i-1} \Delta n_j \right) \left[1 - \exp(-\gamma E T_i) \right] \quad (10)$$

where γ is a sensitivity constant associated with the DCG material, E is the exposure intensity of the laser beam, and Δn is the modulation index value achieved for each exposure; also, Δn_{\max} , the maximum index modulation that can be achieved in DCG holographic material, assumes a value of 0.2. Therefore, the exposure of the i 'th hologram is dependent on the exposure parameters of all previously exposed ($i - 1$) holograms. Based on the gelatin waveguide and exposure parameters used in our experiments, we estimate that a maximum of ~ 300 multiply exposed gratings can be fabricated before the modulation index response of the locally sensitized PMSW begins to saturate.

The angular selectivity of our device structure, calculated using Eqs. (5) through (9), is shown in Fig. 6. The diffraction angles are chosen such that all curves are normalized to unity for fixed index modulation Δn . To achieve maximum efficiency at other diffraction angles, Δn can be adjusted. The dependence of the angular width and fanout channel density, as a function of grating interaction length and diffraction angle, are shown in Fig. 7. In this case, the modulation index for each individual waveguide hologram was fixed at a value of 0.01. A mode effective index of $N_{\text{eff}} = 1.517$, a waveguide thickness of $t = 3 \mu\text{m}$, and a center wavelength of $\lambda = 632.8 \text{ nm}$ were also used in the calculation. As seen from Fig. 7, a decrease in angular bandwidth can be achieved by increasing either the grating interaction length or the corresponding Bragg angle. In comparison to waveguide-based devices, where light propagation occurs within the plane of the waveguide layer over large dis-

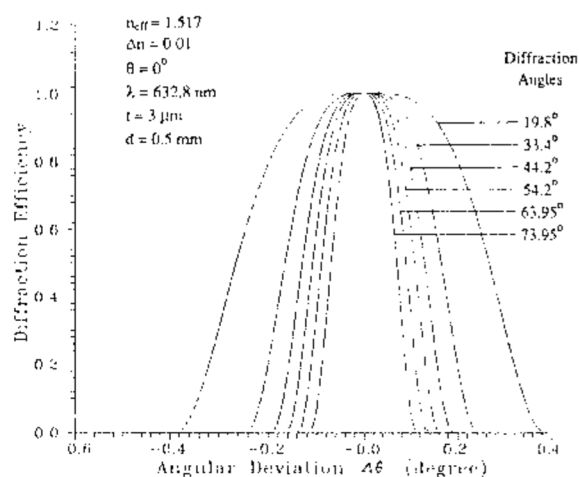


Fig. 6. Angular selectivity for TE guided wave at different diffraction angles.

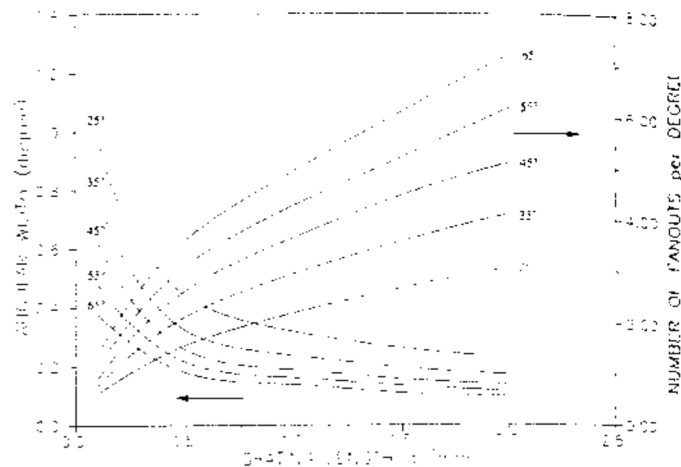


Fig. 7. Angular bandwidth and fanout density, plotted as a function of grating interaction length d . Mode effective index $N_{\text{eff}} = 1.517$, center wavelength $\lambda = 632.8 \text{ nm}$, and waveguide thickness $t = 3 \mu\text{m}$ were used in the calculation.

tances, the smaller interaction lengths ($< 60 \mu\text{m}$) of bulk holographic 1-to- N fanouts and WDM devices^{12,13} actually preclude the achievement of very high channel densities. Based on the above calculations, a maximum channel density of ~ 7 fanouts per degree can be expected for a grating interaction length of 2 mm and a Bragg diffraction angle of 65 deg. We note that, by virtue of the polymer material and waveguide geometry, the interaction length can vary from millimeters to centimeters in dimension. Hence, the modulation index needed to form a high-efficiency deflection device in PMSWs is smaller than in corresponding bulk holographic devices. For example, an interaction length of 0.5 mm would require a modulation index of only $\sim 4 \times 10^{-4}$ in order to achieve 100% diffraction efficiency at an angle of 30 deg. Since the fanout density is largely dependent on the maximum modulation index of the material, DCG is expected to outperform other photorefractive materials, such as Fe-doped LiNbO_3 and SBN, which can achieve maximum modulation indices that are, at best, two to three orders of magnitude smaller.

5. DISCUSSION AND APPLICATIONS

Utilizing the aforementioned high modulation index and refractive index tuning capabilities of the PMSW structure, a number of applications and areas for future development can be considered. For example, in an effort to increase the speed of data transmission and the fanout density in board-to-board interconnection schemes, PMSWs and their holographic fanout elements can be used as the backplane optical interconnects. As described in previous sections, the strength of the polymer waveguide system lies in its ability to be deposited on virtually any kind of smooth substrate surface. Therefore, it should be possible to deposit the PMSW on a backplane substrate that serves as the main interconnection hub between multiple IC boards. If increased parallelism and enhanced interconnect capabilities are required, several integrated PMSW backplanes could then be added to the same board. Future work in this area will continue to emphasize the integration of PMSWs and multiplexed holograms with other optical components, such as coherent sources and photodetectors, to produce polymer-based optoelectronic systems that can simultaneously transmit, route, and receive optical signals. The feasibility of constructing an active waveguide device based on the PMSW reported herein has also been

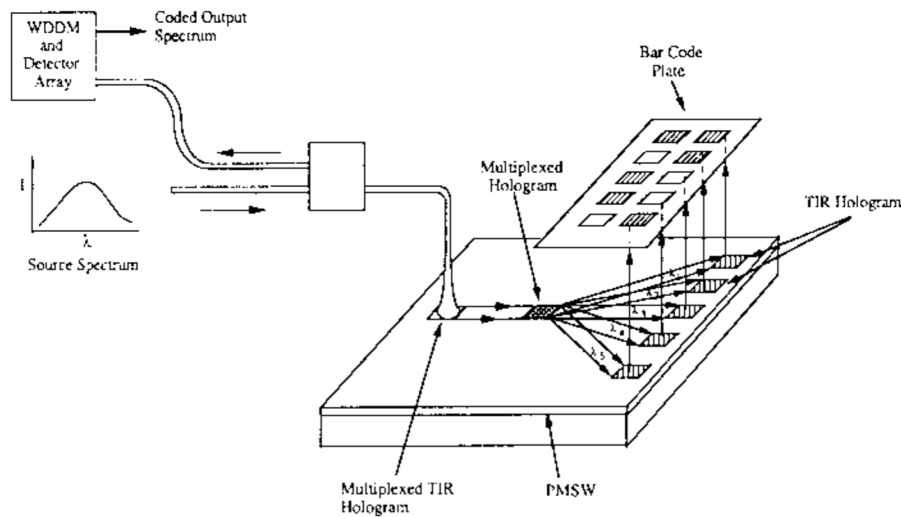


Fig. 8. Schematic of a WDM system used to disperse a broadband signal in a binary code scanning fiber sensor.

successfully demonstrated using a heterowaveguide structure^{14,15} of PMSW/ $\text{In}_x\text{Sn}_{1-x}\text{O}_y$ /PMSW. By introducing highly conjugated noncentrosymmetric (HCNC) molecules into the photo-lime gelatin, an active device based on either $\chi^{(2)}$ or $\chi^{(3)}$ can also be realized. The integration of holographic lenses and highly multiplexed Bragg holograms within the PMSW structures should also facilitate an increase in the number of communication channels that can be used in coherent communication systems. Local area networks, highly parallel computer interconnections, and high-speed long-distance communications are some of the areas in which polymer-based WDDM devices will find applications.

Another application for PMSWs and their corresponding components is in the area of WDM-based fiber optic sensors. For example, WDM techniques can be used to perform operations such as rotary and linear position sensing, rotary speed sensing, and pressure and temperature sensing. In such an application, the WDM or WDDM device might be used as a dispersive element to select a single wavelength signal for subsequent processing. The topology of a novel sensor design is shown in Fig. 8. After the WDM has selected a particular wavelength signal, the light beam is focused onto binary-encoded tracks, whose different binary codes correspond to particular linear, or rotary, sensed parameters. A transmitted beam, for example, might denote a binary 1, while a reflected beam might correspond to a binary 0. The detected optical signal would then be coupled back into a fiber through the same WDM device. In this case, the PMSW-based WDDM would be an excellent choice for demonstrating such an application. In fact, the four-channel WDDM already developed could be used as a linear or rotary position sensor for sensing up to 16 different positions. Each individual position would then be identified by four different binary codes. A four-bit position sensor, as described above, and identified by the binary codes (1,1,0,1) and (1,0,1,1), is depicted in Fig. 9. We note that a 15-channel WDDM sensor, which is capable of providing up to 15-bit binary code sensing capability, is presently under development. This should significantly upgrade the resolution of present fiber sensor systems by more than 30 dB.

6. CONCLUSIONS

We have demonstrated the ability to create low-loss (<1 dB/cm) waveguides in a newly developed polymer microstructure

material using a reproducible refractive index profile tuning method. The deposition of large area (>400 cm²), graded-index polymer waveguides on a variety of substrates, including semiconductors, conductors, insulators, and ceramics, has also been described. The polymer has a transmission bandwidth in excess of 2000 nm, an insensitivity to temperature changes exceeding 280°C and, the ability to realize large index modulations (~ 0.2). A local sensitization process has been used, in conjunction with a holographic recording process, to produce for the first time multiplexed phase gratings and a four-channel wavelength division demultiplexer device in the PMSW films. The ability to fabricate guided-wave devices on any type of substrate, locally

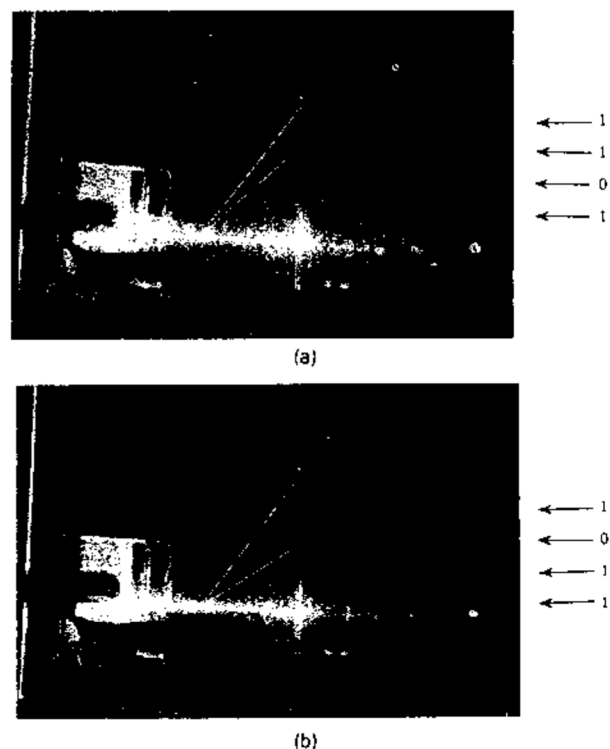


Fig. 9. A four-bit position sensor. The transmission (reflection) of a Bragg diffracted beam in one of the four WDDM channels is denoted by a binary 1 (0) to yield codes of (a) (1101) and (b) (1011).

define passive and active optical components, and potentially achieve a massive 1-to-N fanout density makes the PMSW an attractive candidate and key element for use in high-density optoelectronic and optically interconnected systems in the visible and infrared spectral regions. Further improvements in waveguide uniformity, propagation loss, and fanout density are expected as refinements in process control and index modulation are implemented.

7. ACKNOWLEDGMENT

This research project was sponsored by the SBIR program office of the Strategic Defense Initiative Office (SDIO), contract DASG60-89-C-0053.

8. REFERENCES

1. R. T. Chen, "Polymer waveguide in conjunction with integrated holographic optical elements on GaAs, LiNbO₃, glass, and aluminum substrates for optical interconnects, signal processing, and computing," in *Optical Information Processing Systems and Architectures*, Proc. SPIE 1151, 618-71 (1989).
2. R. T. Chen, W. Phillips, T. Jansson, and D. Pelka, "Integration of holographic optical elements with polymer gelatin waveguides on GaAs, LiNbO₃, glass, and aluminum substrates," *Opt. Lett.* 14, 892-894 (1989).
3. R. T. Chen, M. R. Wang, and T. Jansson, "Polymer microstructure waveguides on alumina and beryllium oxide substrates for optical interconnection," *Appl. Phys. Lett.* 56, 709-711 (1990).
4. J. D. Jackson, *Classical Electrodynamics*, John Wiley & Sons, New York (1980).
5. P. K. Tien, R. Ulrich, and R. J. Martin, "Modes of propagating light waves in thin deposited semiconductor films," *Appl. Phys. Lett.* 14, 29 (1969).
6. J. M. White and P. F. Heidrich, "Optical waveguide refractive index profiles determined from measurement of mode indices: a simple analysis," *Appl. Opt.* 15, 151-155 (1976).
7. B. J. Chang and C. D. Leonard, "Dichromated gelatin for the fabrication of holographic optical elements," *Appl. Opt.* 18, 2407-2417 (1979).
8. M. R. Wang, R. T. Chen, G. J. Sonek, and T. Jansson, "Wavelength division multiplexing and demultiplexing on locally sensitized single-mode polymer microstructure waveguides," *Opt. Lett.* 15, 363-365 (1990).
9. H. Kogelnik, "Coupled wave theory for thick hologram gratings," *Bell Syst. Tech. J.* 48, 2909-2947 (1969).
10. R. P. Kozan, "Theory of diffraction of guided optical waves by thick holograms," *J. Appl. Phys.* 46, 4545-4551 (1975).
11. A. C. Walker, M. R. Tughzudch, J. G. H. Mathew, I. Redmond, R. J. Campbell, S. D. Smith, J. Dempsey, and G. Lebreton, "Optically bistable thin-film interference devices and holographic techniques for experiments in digital optics," *Opt. Eng.* 27, 38-44 (1988).
12. T. Jansson and J. Jannson, "High efficiency Bragg holograms in the IR, visible, UV, and XUV spectral regions," in *Holographic Optics: Design and Applications*, Proc. SPIE 883, 84-93 (1984).
13. R. T. Chen, M. R. Wang, F. Lin, and T. Jansson, "Thick phase hologram for optical clock distribution applications on wafer scale integrated circuits," in *Photopolymer Device Physics, Chemistry, and Applications*, Proc. SPIE 1213, 27-31 (1990).
14. R. T. Chen, I. Sadovnik, T. Jansson, and J. Jansson, "Single-mode polymer waveguide modulator," *Appl. Phys. Lett.*, Vol. 58, 1-3 (1991).
15. Ray T. Chen, "A solution to very high speed integrated circuits and systems," in *Integrated Optical Circuits*, Proc. SPIE 1374 (1990).

Ray T. Chen received his Ph.D. degree in electrical engineering from the University of California, Irvine, in 1988, under the direction of Professor Chen S. Tsai. He received his MS and BS degrees in physics from University of California, San Diego, and National Tsing-Hua University, Taiwan, in 1983 and 1980, respectively. He is currently the director of electro-optic engineering at Physical Optics Corporation. He has been the principal investigator and program manager of over 10 DOD, NSF, and private industrial programs covering integrated optics, passive and reconfigurable optical interconnects, electro-optic switches, polymer waveguides and waveguide modulators, WDMs, optical sensors, switching networks for fiber sensor arrays, image processing, holographic optical elements, and lithography. He also has four domestic patents pending on optics-related technologies. Dr. Chen has more than 40 publications in the open literature. He is a member of SPIE, OSA, IEEE, and Photonics Society of Chinese-Americans (PSC).

Michael R. Wang received both the BS and MS degrees in physics and is currently a Ph.D. candidate in the Department of Electrical and Computer Engineering at University of California, Irvine. Since 1989, he has also been associated with the Physical Optics Corporation as a research scientist. His main research interests include integrated optics, optoelectronics, holographic optical elements, and optical interconnects. Mr. Wang is a member of SPIE and OSA.

Gregory J. Sonek received the BS degree in physics from the Polytechnic Institute of New York, and the MS and Ph.D. degrees in applied physics from Cornell University in 1979, 1982, and 1986, respectively. Since 1986, he has been an assistant professor of electrical and computer engineering at the University of California, Irvine. Dr. Sonek's primary research interests are in the areas of electro-optic and semiconductor guided-wave devices, quantum electronics, and optical laser trapping phenomena for biomedical applications.

Tomasz Jansson: Biography and photograph unavailable.